Digestive Diseases and Sciences (2023) 68:1306–1315
https://doi.org/10.1007/s10620-022-07751-x

ORIGINAL ARTICLE

Chromosome 12 Open Reading Frame 49 Promotes Tumor Growth and Predicts Poor Prognosis in Colorectal Cancer

Yiming Tao[1,2] · Jia Luo[3] · Hongyi Zhu[4,5] · Yi Chu[4,5] · Lei Pei[6]

Received: 16 August 2022 / Accepted: 25 October 2022 / Published online: 8 November 2022

Abstract

Background and Aims Little is known about the role of chromosome 12 open reading frame 49 (C12ORF49)-induced metabolic signal transduction in tumor growth. We investigated the relationship between C12ORF49 expression and prognosis in colorectal cancer (CRC) patients.

Methods C12ORF49 protein expression was measured in CRC tissues by Western blot and immunohistochemistry staining. Knock out of C12ORF49 in CRC cells was then performed, and the role of C12ORF49 in CRC cell proliferation and growth was examined. The expression of C12ORF49 in CRC was analyzed in Gene Expression Profiling Interactive Analysis (GEPIA) databases. A prognosis model with 11 C12ORF49-associated genes (CAGs) was generated by TCGA databases.

Results C12ORF49 expression was significantly higher in CRC tumor tissue than in non-tumor tissue. Furthermore, in vitro and in vivo loss-of-function experiments, showed that C12ORF49 plays critical roles in promoting tumor cell growth. There was a significant correlation between C12ORF49 protein and the presence of tumor necrosis. C12ORF49 is critical for its interaction with SREBF1, TMEM41A, and S1PR3 in the poor prognosis of CRC.

Conclusions Our results suggest that C12ORF49 plays a key role in CRC tumor growth.

Keywords C12ORF49 · Colorectal cancer · Lipid metabolism · Tumor necrosis · Prognosis

Introduction

Colorectal cancer (CRC) is a major issue for global health, with 576,858 colorectal cancer deaths in 2020 [1]. The tumor microenvironment exhibits the necessary prerequisite for CRC progression and metastasis. As a tumor microenvironment key indicator, tumor necrosis (TN) has been proven to be a promoter of angiogenesis, growth, hypoxia, inflammatory responses, and metabolic stress [2–5]. The prognostic value of TN has been reported as a poor marker for CRC patients [6]. Nevertheless, the regulatory mechanism of TN has rarely been examined in CRC [7].

A relationship between lipid metabolism at the proliferation of most cancers has been confirmed [8]. Chromosome 12 open reading frame 49 (C12ORF49, also termed SPRING1) has a vital regulatory role in cholesterol and fatty acid metabolism [9, 10]. Recent studies have demonstrated that C12ORF49 is involved in activating the sterol regulatory element-binding protein (SREBPs) pathway by interacting with S1PR3 and TMEM41A [11, 12]. Emerging evidence implies a strong association between the C12ORF49 signal pathway and cancer pathogenesis. However, little is

✉ Lei Pei
peilei@csu.edu.cn

1 Department of General Surgery, Xiangya Hospital, Central South University, Changsha 410008, Hunan, China

2 National Clinical Research Center for Geriatric Disorders, Xiangya Hospital, Central South University, Changsha 410008, Hunan, China

3 Department of Surgery, Hunan Cancer Hospital, Affiliated Tumor Hospital of Central South University, Changsha 410013, Hunan, China

4 Department of Gastroenterology, The Second Xiangya Hospital, Central South University, Changsha 410011, China

5 Research Center of Digestive Disease, Central South University, Changsha 410011, Hunan, China

6 Department of General Surgery, The Second Xiangya Hospital, Central South University, No.139 Renmin Road, Changsha 410011, China

known about its role in promoting tumor growth and tumor necrosis. Here, we investigate the expression of C12ORF49 in CRC cell lines and CRC tissues.

Materials and Methods

Ethical Approval

All clinical tissue samples used in this investigation were in accordance with the principles in the Declaration of Helsinki. Procedures were conducted with experimental practices approved by the ethics committee of The Second XiangYa Hospital, Central South University, China (permit number 2019112).

Patient Tissue Collection

Paired CRC tissues and noncancerous tissues ($n = 68$) that underwent surgical resection between May 2019 and August 2020 were randomly collected from The Second XiangYa Hospital, Central South University, China. Before surgery, all individuals gave informed consent for the use of their tissues in scientific research.

Histopathological Evaluation of Tumor Necrosis

The tumor necrosis phenotype was defined as erosion or ulceration of a tumor on endoscopy or gross morphology, or necrotic appearance of tumor cells in the whole tumor area, with or without infiltrating inflammatory cells in the stroma on histologic examination [7, 13]. We defined patients with any these tumor necrosis characteristics as "tumor necrosis," and the remaining patients as "without tumor necrosis."

Cell Lines and Culture Reagents

Seven human CRC cell lines (LoVo, HCT116, SW620, SW480, CACO-2, HT-29, and SW40), and one normal colon epithelial cell line (NCM-460) were used in this study. The cell lines were purchased from the Cell Bank Center (Chinese Academy of Sciences, Shanghai, China). Cell culture protocols followed the supplier's suggestions. Cells were cultured in RPMI-1640 (Gibco, Carlsbad, CA) with 10% fetal bovine serum at 37°C in 5% CO_2.

Establishment of C12ORF49-Knockout CRC Cell Lines

The CRISPR/Cas9 system was used to established C12ORF49-deficient LoVo cells. Single guide RNA (sgRNA) sequences were: 5′–ACGATACAAGGCTGTTAG AGAG′; and bottom strand sequences were: 5′–TACGTC CAAGGTCGGGCAGGAAG–3′. For control cells, no guide RNA was inserted. The gRNA sequences were selected according to a standard protocol. In vitro and in vivo tumor growth assays were performed using the CRC cell line LoVo.

Cell Proliferation Assay

LoVo cells were plated at density of 800 cells per well. The Cell Counting Kit-8 (Roche, Germany, cat. no. 11465007001) was used to measure cell proliferation according to the manufacturer's protocol. Each independent cell count was performed in triplicate.

Colony-Forming Assay

In six-well plates, 1000 cells were plated in each well, and colonies of LoVo cells were stained with 0.2% crystal violet (Beyotime, China, cat. no. C0121). After incubation for 14 days, each independent colony experiment was repeated in triplicate.

Immunohistochemistry (IHC)

IHC staining was done as previously described [14]. Following incubation with primary antibodies C12ORF49 (Cat. no. ab211634, Abcam,1:500) and p-STAT3 (phospho-Tyr705) (cat. no. 9131, Cell Signaling Technology, 1:500) were used. The IHC score was calculated by multiplying the staining intensity by percentage of positive cells. Low expression of C12ORF49 was defined as a total staining score < 2, while high expression of C12ORF49 was defined as a total staining score ≥ 2. Stained CRC tissue sections were examined independently by two independent pathologists.

Tumor Xenograft Mice Models Experiments

All subcutaneous CRC mouse model protocols were approved by the Animal Care and Use Committee at Central South University, China. C12ORF49-knockout LoVo cells were injected subcutaneously into the left axilla (2×10^6 cells/mouse, 200 μL). All nude mice were sacrificed under general anesthesia.

Western Blot

Proteins were extracted using RIPA lysis buffer (cat. no. 20-188, Merck, MA, USA). CRC cells were lysed by RIPA lysis buffer supplemented with protease inhibitors (Roche). The protein concentration of CRC cells was measured by the BCA protein assay kit (cat. no. 23225, Pierce, IL, USA). After determination of the protein concentration, lysates (50 μg) were separated by 4–12% Tris–HCl precast SDS-PAGE gels (Bio-Rad). Subsequently, proteins separated by denaturing polyacrylamide gel were transferred

electrophoretically onto an NC membrane (Millipore, USA). Then, the NC membranes were blocked in 5% Tris-Buffered Saline Tween-20 (TBST) and probed with one of the following primary antibodies: C12ORF49 (cat. no. ab211634, Abcam,1:1000), SREBP1 (cat. no. 28481, Abcam, 1:1000), TMEM41A (cat. no. A61422-100, Epigentek, 1:1000), or S1PR3 (cat. no. PAB25114, Abnova, 1:1000). The following day, the membranes were incubated with anti-mouse or rabbit immunoglobulin G (IgG) (HRP) secondary antibody (Thermo Fisher Scientific). Finally, bound secondary antibodies nitrocellulose membranes were detected by the Western Blotting enhanced chemiluminescence (ECL) kit.

Online Bioinformatics Analysis

High C12ORF49 expression in CRC relative to noncancerous tissues was confirmed by Gene Expression Profiling Interactive Analysis (GEPIA) online database web servers (http://gepia.cancer-pku.cn/) [15]. The correlation between C12ORF49 and STAT3 was identified by the TIMER online database (https://cistrome.shinyapps.io/timer/) [16]. The expression profiles of C12ORF49 mRNA in various human CRC cells were obtained from the DepMap portal database, including CRISPRi (CERES) and RNAi (DEMETER) screens (https://depmap.org/portal/) [17]. C12ORF49 gene dependency represented by probability of knocking out a gene has a real depletion effect.

Construction of a Prognostic C12ORF49-Associated Gene Signature

We used Lasso regression to generate a final prognosis model with 11 C12ORF49-associated genes (CAGs), including *TMEM41A*, *S1PR3*, *AKT2*, *SREBF1*, *MBTPS1*, *SCD*, *AKT2*, *S1PR2*, *SREBF2*, *S1PR1*, and *MBTPS2*. To reduce the dimensionality and select the CAGs, the Lasso method was used. A prognostic risk score based on the CAGs was calculated as follows: min risk score = (0.504)*SPRING1 + (0.2175)* SREBF1 + (0.3057)* TMEM41A + (0.3065)* S1PR3.

Statistical Analysis

Statistical analysis and graphs of experimental data were performed using GraphPad Software 9.0 (San Diego, CA, USA). The reported data are at least three replicates of three independent experiments . ANOVA with Tukey's multiple comparisons tests were performed. We considered calculated probabilities significant at $P < 0.05$.

Table 1 Clinicopathological variables and their correlation with immunohistochemical expression of C12ORF49 in CRC patients

Clinicopathological variables	*n*	C12ORF49 expression		*P*-value
		Low (*n* = 27)	High (*n* = 41)	
Age				
< 55	31	10	21	0.3220
≥ 55	37	17	20	
Gender				
Male	33	14	19	0.8047
Female	35	13	22	
Primary tumor location				
Colon	39	20	19	0.0273
Rectum	29	7	22	
Differentiation				
High	21	13	8	0.0167
Low-middle	47	14	33	
Tumor diameter				
< 5 cm	33	11	22	0.0385
5–8 cm	20	13	7	
8–10 cm	11	2	9	
≥ 10 cm	4	1	3	
Lymph node metastasis				
Positive	29	13	16	0.6167
Negative	39	14	25	
UICC stage				
I + II	36	19	17	0.0261
III + IV	32	8	24	
Vascular cancer embolus				
Yes	27	9	18	0.4528
No	41	18	23	
Tumor necrosis				
Positive	35	9	26	0.0250
Negative	33	18	15	

Results

Association Between C12ORF49 and Tumor Necrosis

To determine whether C12ORF49 contributes to the progression of CRC, we examined the relative expression levels of C12ORF49, SREBF1, TMEM41A, and S1PR3 proteins in a cohort of 68 paired CRC patients (Fig. 1a). Table 1 provides an overview of clinicopathological variables and their correlation with immunohistochemical expression of C12ORF49 of 68 CRC patients. CRC specimens were divided into two groups: with or without tumor necrosis (Fig. 1b). Western blotting demonstrated that the expression of C12ORF49, SREBF1, TMEM41A, and S1PR3 in CRC tumor tissues significantly correlated with TN (Fig. 1c).

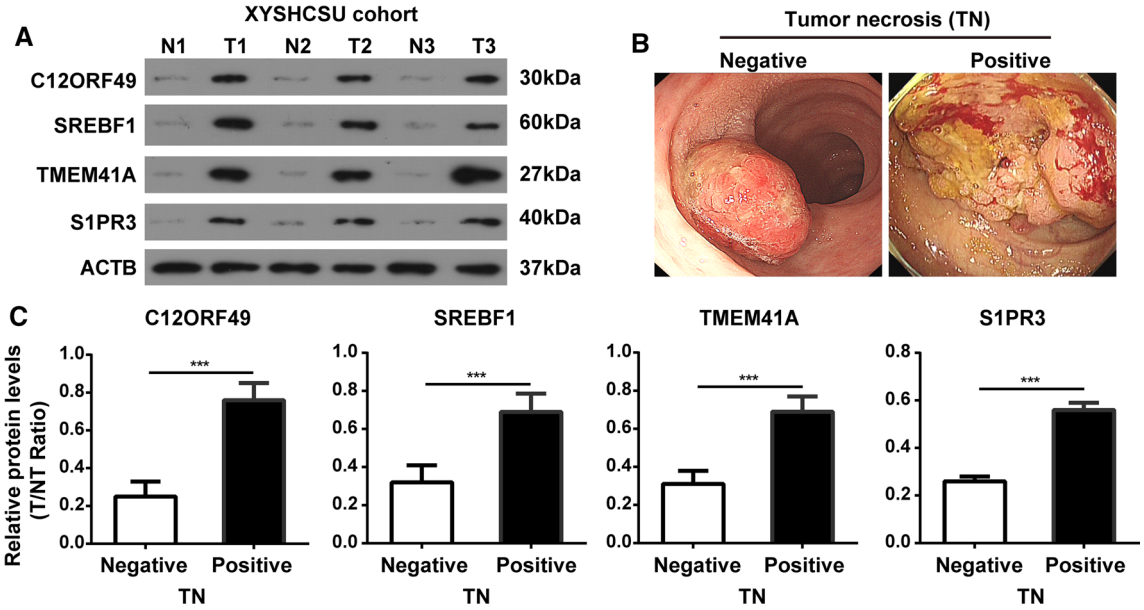

Fig. 1 Increased expression of C12ORF49 protein in human CRC tissues with TN. **a** Representative Western blot images of C12ORF49, SREBF1, TMEM41A, and S1PR3. **b** Representative colonoscopy images of CRC tumor necrosis. **c** Comparative analysis of C12ORF49, SREBF1, TMEM41A, and S1PR3 expression in the presence and absence of tumor necrosis

C12ORF49 Knockout Inhibited CRC Tumor Cell Proliferation and Growth

The mechanisms by which C12ORF49 promotes tumor growth and necrosis remain unknown; therefore, we firstly analyzed the expression profiles in the DepMap portal database, using DepMap's default perturbation effect cutoff of 0.5, and found that perturbation of C12ORF49 in CRC lines causes strong growth retardation (Supplementary Fig. S2).

Protein levels of C12ORF49 among LoVo, HCT116, SW620, SW480, CACO-2, HT-29, and SW40 CRC cell lines were compared with the normal epithelial cell line NCM-460 by Western blot. The expression levels of C12ORF49 were elevated in CRC cell lines compared with NCM-460 (Fig. 2a). CRISPR/Cas9 C12ORF49 knock out LoVo cells were constructed by CRISPR/Cas9 genome editing and the effects of C12ORF49, SREBF1, TMEM41A, and S1PR3 in CRC cells were evaluated. We selected two clones, C12ORF49-KO-1 and C12ORF49-KO-2, for our initial analyses. Knockdown efficiency results were 55% for KO-1 and 70% for KO-2 C12ORF49 mRNA. Knockout of C12ORF49 downregulated SREBF1, TMEM41A, and S1PR3 expression in C12ORF49-deficient LoVo cells (Fig. 2b). The potential of cell proliferation in C12ORF49 knockout CRC cells was slowed down compared with the widetype (WT) cell group (Fig. 2c). Cell colony assays further confirmed the similar suppressive effects of C12ORF49 knockout (Fig. 2d). As expected, C12ORF49 knockout had the same suppressive effects on CRC tumor growth in vivo. The average tumor weights of subcutaneous xenograft animals in the KO-1, KO-2, and WT groups were 0.35 ± 0.09 g, 0.56 ± 0.09 g, and 0.97 ± 0.09 g, respectively (Fig. 2e). These results indicated the knockdown efficiencies of C12ORF49-KO-2 in inhibiting tumor cell proliferation and growth. In agreement with the DepMap exome-wide 20Q2 CRISPR-Cas9 deletion data of C12ORF49-associated genes (CAGs) (Supplementary Fig. S2), C12ORF49 function within tumor cells may exhibit proliferative effects in CRC cells.

Correlation Between C12ORF49 Expression and STAT3

Metabolic stress in the tumor microenvironment associated with tumor growth has commonly been considered the cause of tumor necrosis and inflammation [18, 19]. Therefore, the correlation between C12ORF49 expression and HIF-1α/STAT3/NF-κB signaling was analyzed in the TIMER database (Fig. 3a). In colon adenocarcinoma (COAD) tissues, C12ORF49 expression level had a significantly positive correlation with infiltrating levels of STAT3 ($R = 0.54$, $P < 0.001$), HIF-1α ($R = 0.441$, $P < 0.001$), and NF-κB ($R = 0.354$, $P < 0.001$). In rectal adenocarcinoma (READ) tissues, C12ORF49 expression level had a significantly positive correlation with infiltrating levels of STAT3 ($R = 0.525$, $P < 0.001$), HIF-1α ($R = 0.4$, $P < 0.001$), and

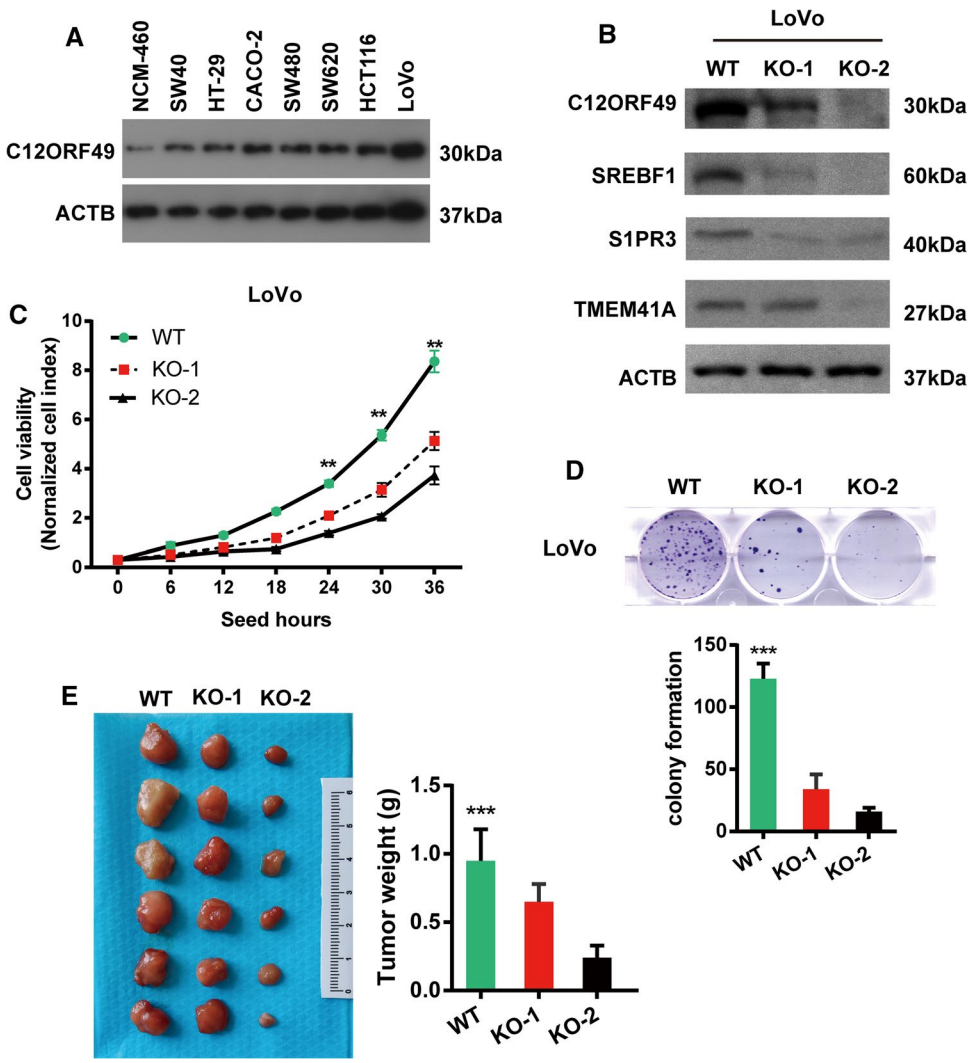

Fig. 2 C12ORF49 knockout inhibits the growth of CRC cells in vitro and in vivo. **a** C12ORF49 protein levels in seven human CRC cell lines were investigated using Western blotting (WB). **b** C12ORF49 knockout effect was confirmed by Western blotting in LoVo cells. The protein level of SREBF1, TMEM41A, and S1PR3 was reduced in C12ORF49-deficient LoVo cells. **c** Cell proliferation assay showed that C12ORF49 knockout slows cell proliferation in LoVo and WT cells. **d** Colony formation assays of C12ORF49-deficient colonies derived from LoVo and WT cells were performed. **e** Representative gross images of transplanted tumors. Tumor weights are summarized in a bar chart

NF-κB (cor = 0.241, $P < 0.001$). To further confirm the crucial role of STAT3, we performed IHC to determine the expression of p-STAT3 in paired CRC tissues ($n = 68$). CRC tissues had significantly higher p-STAT3 protein expression levels than non-tumor tissues (Fig. 3b). Intriguingly, a significant positive correlation between C12ORF49 expression and p-STAT3 activation status was observed in CRC tissues ($P < 0.001$; $R = 0.446$; Fig. 3c). Also, C12ORF49 was positively correlated with immune cell markers among COAD and READ cells in TIMER (Supplementary Table S1).

Association of C12ORF49-Related Signature Genes with Poor Prognosis of CRC

The expression of C12ORF49 genes in colon adenocarcinoma (COAD) and rectal adenocarcinoma (READ) tumors was significantly upregulated compared with in noncancerous tissues, according to the GEPIA database ($P < 0.01$, Fig. 4a). To validate the prognosis value in CRC, we constructed a prognostic risk model to investigate the relationship between COAD prognostics and C12ORF49-associated genes (CAGs). The specific coefficient information of these genes is shown in Fig. 5. Figure 4b shows that C12ORF49 is critical for its interaction with SREBF1, TMEM41A, and S1PR3 in the poor prognosis of CRC. Kaplan–Meier analysis indicated that CRC patients with high CAGs scores had a significantly shorter overall survival (OS) (Fig. 4c). For 1-, 3-, and 5-year overall survival predictions, the time-dependent receiver operating characteristics (ROC) were 0.61, 0.618, and 0.5595, respectively (Fig. 4d), showing that the risk score model can predict the OS for patients.

As demonstrated in Table S2, C12ORF49 expression was related not only to tumor size and lymph metastasis in CRC patients, but also to the treatment method applied. This indicates that C12ORF49 is potentially suitable for selecting patients who will benefit from radiation therapy ($P = 0.006$).

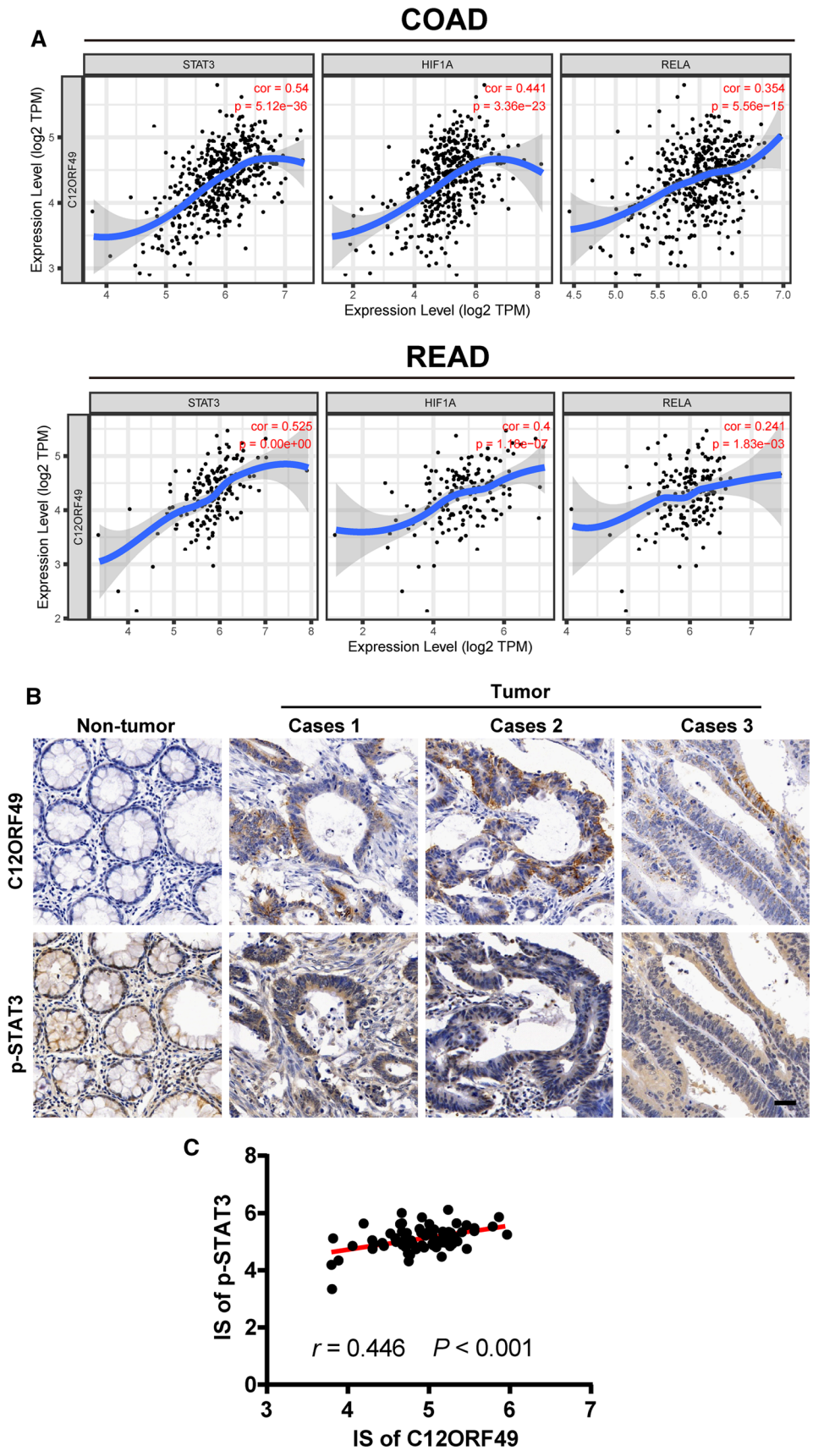

Fig. 3 Involvement of HIF-1α/STAT3/NF-κB signaling in C12ORF49-mediated CRC. **a** Correlation of C12ORF49 expression with immune infiltration level in COAD and READ. **b** The C12ORF49 expression and p-STAT3 were analyzed by IHC in 68 paired CRC samples. **c** A statistically significant positive association of C12ORF49 and p-STAT3 was observed in CRC specimens

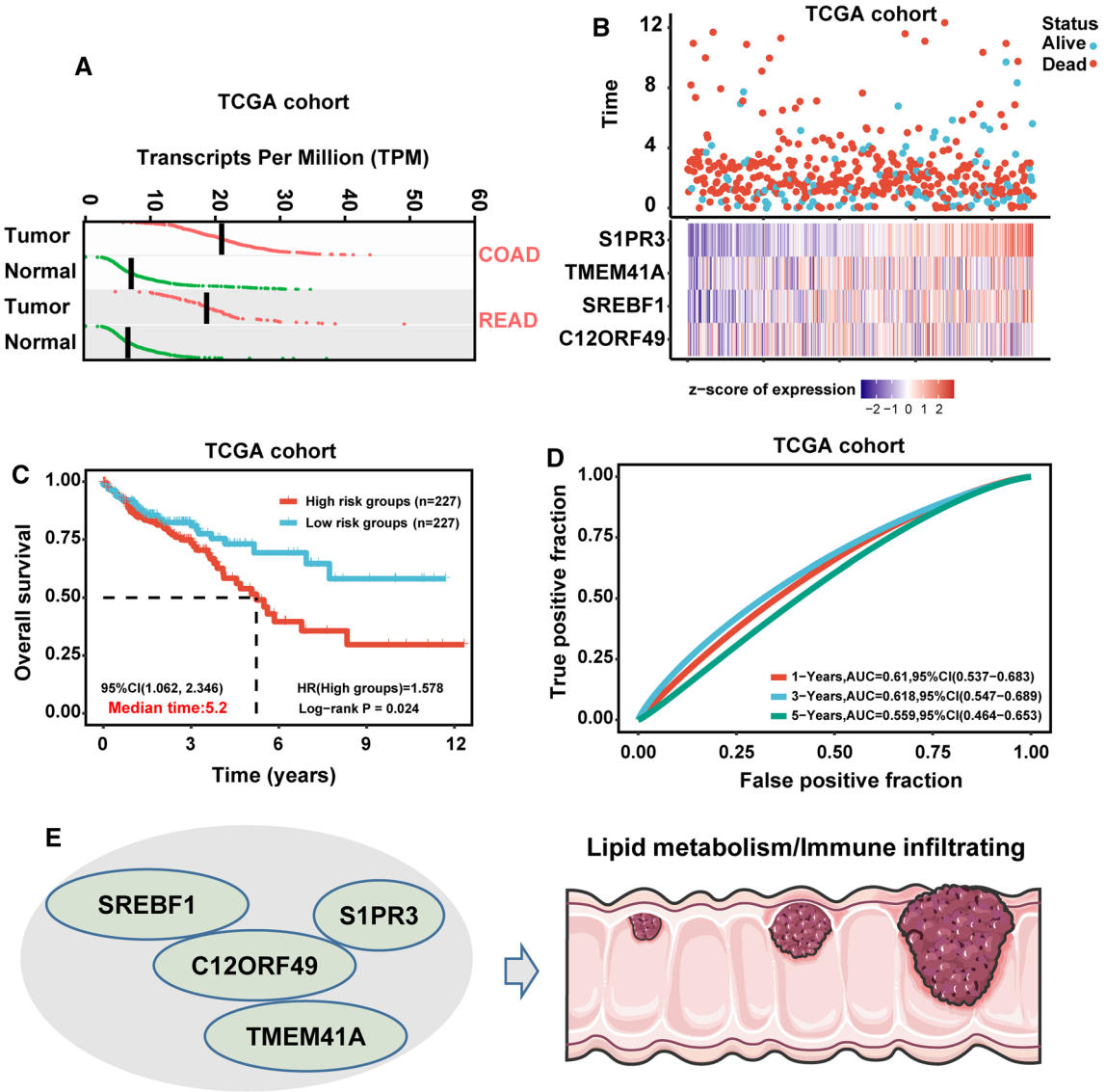

Fig. 4 Identification of C12ORF49-associated genes (CAGs) prediction model for CRC. **a** C12ORF49 mRNA expression in COAD and READ compared with noncancerous tissues obtained from the GEPIA. **b** The correlation between selected CAGs signatures and overall survival was evaluated. **c** The association between overall survival and CAGs risk score model was assessed in TCGA-COAD dataset. **d** Time-dependent ROC curve analysis of the selected CAGs risk signature had a relatively high accuracy. **e** Proposed model of C12ORF49 interacts with SREBP pathway proteins SREBF1, TMEM41A, and S1PR3, and promotes tumor growth in CRC

Based on our data that overexpression of C12ORF49 occurs in CRC cell lines and tumor tissues, we propose that C12ORF49 regulates the SREBP pathway via interaction with SREBF1, TMEM41A, and S1PR3. The interaction of C12ORF49 and the SREBP pathway jointly initiates changes in lipid metabolism and immune infiltration, leading to the growth of CRC (Fig. 4e).

Discussion

This study revealed that C12ORF49 was significantly upregulated in CRC tissues compared with non-tumor tissues. We undertook the experiment to support the hypothesis of the tumor promoting role of C12ORF49 in CRC malignancies. Notably, C12ORF49 signaling may be involved in STAT3 signaling. C12ORF49 was consistently identified as a promoter of CRC by TCGA-sequence databases. These findings contribute to our understanding of the novel role of lipid metabolism C12ORF49 in the regulation of tumor necrosis,

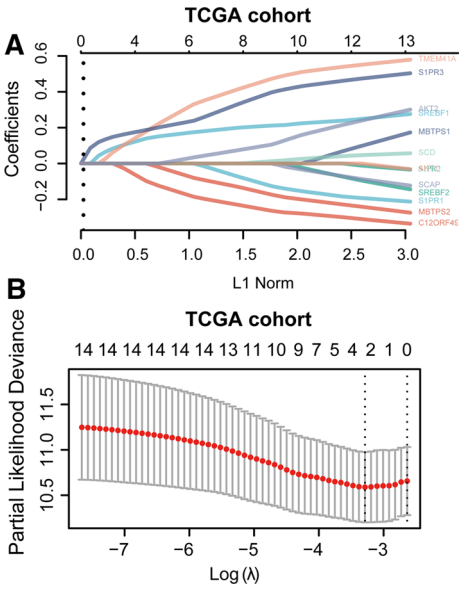

Fig. 5 The prognosis-significant CAGs were selected by the Lasso Cox regression method. **a** Lasso regression was used to narrow the range of prognostic genes, remove overfitting between genes, and calculate risk scores based on the Lasso regression coefficients. **b** The prognosis-significant CAGs selected by the Lasso Cox regression method

and provide a basis for closely linking metabolic stress to necrotic tumor growth.

Tumor necrosis is a prognostic marker for liver cancer [20], lung cancer [18], nasopharyngeal cancer [21], kidney cancer [22], and CRC [6]. Tumor necrosis is believed to occur as a consequence of metabolic stress and inflammation [5]. However, the complicated regulatory mechanisms of tumor necrosis in CRC remain unclear. Here we show for the first time that C12ORF49 and C12ORF49-associated genes were overexpressed in CRC tissues and cell lines. Compared with the non-tumor necrosis CRC patients, elevated levels of C12ORF49 in necrotic tumor were detected. Furthermore, C12ORF49 knockout inhibited the growth of CRC cells, which was confirmed in vitro and in vivo experiments, indicating the vital role of C12ORF49 in tumor growth.

Previous studies have shown that SREBF1 promotes CRC tumor invasion and metastasis via promoting the expression of MMP7. SREBF1 is associated with p65 phosphorylation [23, 24]. Knockdown of TMEM41A was also observed to affect gastric cancer metastasis via the modulation of E-cadherin [25]. Colorectal carcinoma chemoresistance to gemcitabine was induced by SREBP-1-mediated lipogenesis and STAT3 activation in CRC [26]. Consistent with the literature, we found that the interaction of C12ORF49 with SREBF1, TMEM41A, and S1PR3 is critical for the poor prognosis of CRC. This study supports evidence from previous observations on the tumor-promoting role of transcription factors involved in cholesterol and fatty acid synthesis. In view of that, a C12ORF49-associated genes (CAGs) prediction model for CRC was constructed to validate the prognosis value. Kaplan–Meier analysis indicated high CAGs scores had a prognostic value in CRC patients. Current prognosis markers of CRC focus on chromosomal instability, Microsatellite Instability (MSI), or CpG island methylation molecular pathways, which greatly widen the molecular basis of CRC [27]. However, their clinical prognostic or predictive to therapy value remains to be examined through randomized control trials. Our investigation suggests that C12ORF49-associated genes might have potential prognostic value for predictive markers of radiotherapy benefits. We will focus on the reliability and predictive value in the future.

Accumulating evidence has revealed that CRC is a malignancy characterized by inflammation and immunopathogenesis. Many studies have shown that STAT3 and NF-κB have key roles in colon carcinogenesis and inflammation, which subsequently contributes to activating macrophages [28]. Our study found that C12ORF49 is closely correlated with NF-κB activity in CRC. In addition, we found that C12ORF49 enhanced HIF-1α/STAT3/NF-κB activity, elucidating a novel C12ORF49-driven signaling pathway.

Although C12ORF49 is a central regulator involved in lipid metabolism, how C12ORF49 drives CRC cell survival and its function in apoptosis is less well understood. Lipotoxic cell death was previously linked to inflammation in cancer initiation and development, with the interplay between HIF-1α and inflammation signaling pathways in the hypoxic tumor microenvironment having been established [29]. HIF-1α has been reported to regulate cell metabolism [30]. In this study, a positive relationship between C12ORF49 and HIF-1α/STAT3 was observed. Indeed, the STAT3/NF-κB pathway can cross-talk with PI3K and AKT signaling in CRC progression [31–33]. These studies further our understanding of the novel role of lipid metabolism target C12ORF49 in CRC with tumor necrosis. This observation may support the hypothesis that C12ORF49 may release pro-inflammatory factors and in the activation of NF-κB, triggers an immunosuppressive microenvironment and promotes cancer progression.

Our observations identified C12ORF49 as a novel biomarker that may be an effective therapeutic target of CRC. This discovery significantly increases current knowledge about the role of lipid metabolism in inflammation-driven cancer. Future studies are required to explore C12ORF49 functions in these signaling pathways.

Supplementary Information The online version contains supplementary material available at https://doi.org/10.1007/s10620-022-07751-x.

Author's contribution L.P. designed the research, conceived the study design, supervised the major project, and revised the manuscript throughout this study. Y.M.T. performed the functional experiments, carried out the data analysis and composed the figures, and wrote the final manuscript. J.L. participated in study design and helped to draft the manuscript. H.Y.Z. and Y.C. participated in the clinical sample experiments and performed the statistical analysis. All authors read and approved the final manuscript.

Funding This study was supported by the grants from the National Nature Science Foundation of China (No. 81502545, 81372630, U20A20408, 82074450).

Declarations

Conflict of interest All authors have read manuscript and then approved the submitted manuscript. All authors also have declare no competing interests or other financial competing interests.

References

1. Sung H, Ferlay J, Siegel RL et al. Global Cancer Statistics 2020: GLOBOCAN Estimates of Incidence and Mortality Worldwide for 36 Cancers in 185 Countries. *CA: a cancer journal for clinicians.* 2021;71:209–249.
2. Karsch-Bluman A, Benny O. Necrosis in the tumor microenvironment and its role in cancer recurrence. *Advances in experimental medicine and biology.* 2020;1225:89–98.
3. Lee SY, Ju MK, Jeon HM et al. Regulation of tumor progression by programmed necrosis. *Oxidative medicine and cellular longevity.* 2018;2018:3537471.
4. Su Z, Yang Z, Xu Y, Chen Y, Yu Q. Apoptosis, autophagy, necroptosis, and cancer metastasis. *Molecular cancer.* 2015;14:48.
5. Yee PP, Li W. Tumor necrosis: a synergistic consequence of metabolic stress and inflammation. *BioEssays: news and reviews in molecular, cellular and developmental biology.* 2021;43:e2100029.
6. Komori K, Kanemitsu Y, Kimura K et al. Tumor necrosis in patients with TNM stage IV colorectal cancer without residual disease (R0 Status) is associated with a poor prognosis. *Anticancer research.* 2013;33:1099–1105.
7. Zhang X, Chen L. The recent progress of the mechanism and regulation of tumor necrosis in colorectal cancer. *Journal of cancer research and clinical oncology.* 2016;142:453–463.
8. Bian X, Liu R, Meng Y, Xing D, Xu D, Lu Z. Lipid metabolism and cancer. *The Journal of experimental medicine*. 2021;218.
9. Aregger M, Lawson KA, Billmann M et al. Systematic mapping of genetic interactions for de novo fatty acid synthesis identifies C12orf49 as a regulator of lipid metabolism. *Nature metabolism.* 2020;2:499–513.
10. Bayraktar EC, La K, Karpman K et al. Metabolic coessentiality mapping identifies C12orf49 as a regulator of SREBP processing and cholesterol metabolism. *Nature metabolism.* 2020;2:487–498.
11. Loregger A, Raaben M, Nieuwenhuis J et al. Haploid genetic screens identify SPRING/C12ORF49 as a determinant of SREBP signaling and cholesterol metabolism. *Nature communications.* 2020;11:1128.
12. Xiao J, Xiong Y, Yang LT et al. POST1/C12ORF49 regulates the SREBP pathway by promoting site-1 protease maturation. *Protein & cell.* 2021;12:279–296.
13. Cerar A, Zidar N, Vodopivec B. Colorectal carcinoma in endoscopic biopsies; additional histologic criteria for the diagnosis. *Pathology, research and practice.* 2004;200:657–662.
14. Tan F, Zhu H, Tao Y et al. Neuron navigator 2 overexpression indicates poor prognosis of colorectal cancer and promotes invasion through the SSH1L/cofilin-1 pathway. *Journal of experimental & clinical cancer research : CR.* 2015;34:117.
15. Tang Z, Li C, Kang B, Gao G, Li C, Zhang Z. GEPIA: a web server for cancer and normal gene expression profiling and interactive analyses. *Nucleic acids research.* 2017;45:W98-w102.
16. Li T, Fan J, Wang B et al. TIMER: A Web Server for Comprehensive Analysis of Tumor-Infiltrating Immune Cells. *Cancer research.* 2017;77:e108–e110.
17. Tsherniak A, Vazquez F, Montgomery PG et al. Defining a cancer dependency map. *Cell.* 2017;170:564-576.e516.
18. Alcaraz J, Carrasco JL, Millares L et al. Stromal markers of activated tumor associated fibroblasts predict poor survival and are associated with necrosis in non-small cell lung cancer. *Lung cancer (Amsterdam, Netherlands)* 2019;135:151–160.
19. Hou J, Zhao R, Xia W et al. PD-L1-mediated gasdermin C expression switches apoptosis to pyroptosis in cancer cells and facilitates tumour necrosis. *Nature cell biology.* 2020;22:1264–1275.
20. Ling YH, Chen JW, Wen SH et al. Tumor necrosis as a poor prognostic predictor on postoperative survival of patients with solitary small hepatocellular carcinoma. *BMC cancer.* 2020;20:607.
21. Liang SB, Chen LS, Yang XL et al. Influence of tumor necrosis on treatment sensitivity and long-term survival in nasopharyngeal carcinoma. *Radiotherapy and oncology : journal of the European Society for Therapeutic Radiology and Oncology.* 2021;155:219–225.
22. Zhang L, Zha Z, Qu W et al. Tumor necrosis as a prognostic variable for the clinical outcome in patients with renal cell carcinoma: a systematic review and meta-analysis. *BMC cancer.* 2018;18:870.
23. Gao Y, Nan X, Shi X et al. SREBP1 promotes the invasion of colorectal cancer accompanied upregulation of MMP7 expression and NF-κB pathway activation. *BMC cancer.* 2019;19:685.
24. Zhang L, Qiao X, Chen M et al. Ilexgenin A prevents early colonic carcinogenesis and reprogramed lipid metabolism through HIF1α/SREBP-1. *Phytomedicine : international journal of phytotherapy and phytopharmacology.* 2019;63:153011.
25. Lin B, Xue Y, Qi C, Chen X, Mao W. Expression of transmembrane protein 41A is associated with metastasis via the modulation of E-cadherin in radically resected gastric cancer. *Molecular medicine reports.* 2018;18:2963–2972.
26. Jin L, Zhu LY, Pan YL, Fu HQ, Zhang J. Prothymosin α promotes colorectal carcinoma chemoresistance through inducing lipid droplet accumulation. *Mitochondrion.* 2021;59:123–134.

27. Herzig DO, Tsikitis VL. Molecular markers for colon diagnosis, prognosis and targeted therapy. *Journal of Surgical Oncology*. 2015.
28. Guo M, Li Z, Huang Y, Shi M. Polysaccharides from Nostoc commune Vaucher activate macrophages via NF-κB and AKT/JNK1/2 pathways to suppress colorectal cancer growth in vivo. *Food & function*. 2019;10:4269–4279.
29. Qureshi-Baig K, Kuhn D, Viry E et al. Hypoxia-induced autophagy drives colorectal cancer initiation and progression by activating the PRKC/PKC-EZR (ezrin) pathway. *Autophagy*. 2020;16:1436–1452.
30. Du W, Zhang L, Brett-Morris A et al. HIF drives lipid deposition and cancer in ccRCC via repression of fatty acid metabolism. *Nature communications*. 2017;8:1769.
31. Lai CY, Yeh KY, Liu BF et al. MicroRNA-21 plays multiple oncometabolic roles in colitis-associated carcinoma and colorectal cancer via the PI3K/AKT, STAT3, and PDCD4/TNF-α signaling pathways in Zebrafish. *Cancers*. 2021;13
32. Xue J, Ge X, Zhao W et al. PIPKIγ regulates CCL2 expression in colorectal cancer by activating AKT-STAT3 signaling. *Journal of immunology research*. 2019;2019:3690561.
33. De Simone V, Franzè E, Ronchetti G et al. Th17-type cytokines, IL-6 and TNF-α synergistically activate STAT3 and NF-kB to promote colorectal cancer cell growth. *Oncogene*. 2015;34:3493–3503.